Instituto Nacional de Investigación y Tecnología Agraria y Alimentaria (INIA)
Available online at www.inia.es/sjar
http://dx.doi.org/10.5424/sjar/2013114-4093

Spanish Journal of Agricultural Research 2013 11(4): 958-967
ISSN: 1695-971-X
eISSN: 2171-9292

# Field analysis of the deterioration after some years of use of four insect-proof screens utilized in Mediterranean greenhouses

A. López-Martínez, D. L. Valera-Martínez*, F. D. Molina-Aiz, A. A. Peña-Fernández and P. Marín-Membrive

*Universidad de Almería. Centro de Investigación en Biotecnología Agroalimentaria BITAL. Ctra. de Sacramento s/n. 04120 Almería, Spain*

## Abstract

The installation of insect-proof screens on greenhouse vents is one of the principal methods of protection against harmful insects for crops. Their main disadvantage lies on their negative effects on natural ventilation and greenhouse microclimate, which have been the focus of studies by several authors. However, few works have analysed the effect of accumulated dust and dirt on these screens. The present study has analysed four anti-insect screens, comparing their geometric characteristics before installation and after three to four years of use. Two negative effects have been observed and quantified: deterioration of the threads that make up the screen and reduction of porosity due to accumulated dirt in the pores. This deterioration over time gives leads to a mean increase in thread diameter of 3.1%, as well to a mean decrease in the pore size of 6.2% and 2.3% in the weft ($L_{px}$) and the warp ($L_{py}$), respectively. In fact, the insect-proof screen porosity (φ) decreased due to the deterioration of the threads by an average of 6.5%, in addition to an average 20.3% reduction due to the accumulation of dirt in the pores, making a total reduction in porosity of 26.8%. This decrease in porosity leads to lower greenhouse ventilation rates, and is therefore detrimental for the greenhouse microclimate. Consequently, it is recommended that insect-proof screens in arid areas such as Almería (Spain), with abundant dust suspended in the atmosphere, be washed monthly using water sprayed at high pressure.

**Additional key words**: insect screens; geometric characterisation; accumulation of dust and dirt.

## Introduction

The installation of insect-proof screens on greenhouse vents is one of the principal methods of protecting crops against harmful insects. They are indispensable in greenhouses in Mediterranean countries where the climatology favours such pests. Greenhouses in Andalusia (Spain) are in fact obliged to install insect-proof screens of at least 10 × 20 threads $cm^{-2}$ on all vents (BOJA, 2007).

Insect-proof screens are designed to prevent the entrance of insects into the greenhouse, and consequently the pore size must be smaller than the size of the smallest harmful insect. Nevertheless, they also prevent the exit of insects that are beneficial for the crop, such as pollinating insects (Teitel, 2007). But reducing the porosity of the mesh also reduces the ventilation rate which increases the temperature and humidity inside the greenhouse (Fatnassi *et al.,* 2002 and 2003).

The most harmful insects for crops in the Mediterranean area, and in particular in the province of Almería, are the following: aphids (*Myzus persicae* Sulzev and *Aphis gossipii* Glover), leaf miners (*Liriomyza* sp.), whitefly (*Trialeurodes vaporariorum* Westwood and

* Corresponding author: dvalera@ual.es
Received: 13-02-13. Accepted: 25-09-13.

Abbreviations used: CFD (computational fluid dynamics); HDPE (high density polyethylene). **Nomenclature**: $D_f$ (thread density according to the manufacturer, threads $cm^{-2}$); $D_h$ (diameter of the threads, μm); $D_{hx}$ (diameter of the weft threads, μm); $D_{hy}$ (diameter of the warp threads, μm); $D_i$ (diameter of the inside circumference of the pore, μm); $D_r$ (thread density measurement, threads $cm^{-2}$); $L_{px}$ (length of the pore in the weft direction, μm); $L_{py}$ (length of the pore in the warp direction, μm); $S_A$ (greenhouse surface area, $m^2$); $S_p$ (area of the pore, $mm^2$); $S_t$ (reference surface area, $mm^2$); $S_V$ (vent surface area ($m^2$). **Greek letters**: φ (porosity, $m^{-2}$ $m^{-2}$); $\varphi^*$ (estimated imaging porosity, $m^{-2}$ $m^{-2}$).

*Bemisia tabaci* Gennadius), thrips (*Frankliniella occidentalis* Pergande and *Thrips tabaci* Lindeman), and a recent arrival in Almería, mealybugs (*Tuta absoluta* Meyrick). As well as producing direct damage to crops, these pests may also transmit phytopathogenic viruses which are extremely damaging to crops (Smith, 1972).

Insect-proof screens must be placed at all greenhouse ventilation openings, and their use contributes to reducing the levels of pest populations, and therefore the incidence of direct damage to the crop and the transmission of diseases. Consequently, greenhouse growers are less likely to need phytosanitary treatments (Baker & Jones, 1989; Berlinger *et al*., 1991 and 1992; Taylor *et al*., 2001; Teitel, 2007), which has a most positive effect on the profitability of the crops and contributes to the reduction of negative environmental impacts. In Israel, Taylor *et al*. (2001) estimated that losses due to *B. tabaci* amounted to 15-32 million dollars between 1980 and 1990, and these could have been avoided if insect-proof screens had been used. However, the main drawback of these screens is their negative effect on natural ventilation and greenhouse microclimate.

Numerous works have studied the characteristics of insect-proof screens and how their use affects the natural ventilation of greenhouses. In the laboratory, several authors have analysed the aerodynamic characteristics of these screens in controlled conditions in wind tunnels (Miguel *et al*., 1997; Dierickx, 1998; Valera *et al*., 2005 and 2006). These characteristics can also be ascertained by means of CFD (Computational Fluid Dynamics) simulations, though the results vary significantly (Valera *et al*., 2005; Teitel, 2010).

The effect of insect-proof screens on ventilation, air temperature and humidity in naturally ventilated greenhouses has been studied previously. The climatic conditions in a naturally ventilated greenhouse depend on the screen's characteristics, the type of vent and on the wind (Miguel & Silva, 2000). The main disadvantage of using this type of screen is that the ventilation rate and the air speed inside the greenhouse are reduced (Kittas *et al*., 2008). Muñoz *et al*. (1999) studied the effect of insect-proof screens (45% porosity) on the natural ventilation of a multi-tunnel greenhouse using the tracer gas method. They compared three types of vents: hinged roof vents with and without screens, and roll-up roof vents with screen. Based on the results obtained, they recommend using roll-up roof vents that cover almost the whole greenhouse in order to compensate for the screen-induced reduction in ventilation. As the porosity of the screens decreases, so does the ventilation rate, while the greenhouse temperature and humidity rise (Fatnassi *et al*., 2002 and 2003). Using CFD simulations of an Almería-type greenhouse, Baeza *et al*. (2009) concluded that an insect-proof screen (28% porosity) can cause a 77-87% reduction in the ventilation rate.

The installation of insect-proof screens can cause a two-fold increase (41% porosity) or three-fold increase (20% porosity) in the temperature and humidity difference between inside and outside the greenhouse compared to a greenhouse without screens (Fatnassi *et al*., 2006). Bartzanas *et al*. (2002) used CFD simulations to study the effect of a 53% porosity screen on the natural ventilation of a tunnel greenhouse with side vents. This screen caused a 50% fall in the ventilation rate and a 4°C increase in inside temperature. Harmanto *et al*. (2006) used balances of energy and water vapour to study the effect of screens of three different porosities (41, 38 and 30%) on ventilation. In comparison with the most porous screen ($\varphi = 41\%$), the least porous one reduced the ventilation rate by 50% and increased the inside temperature by 3°C, while the other screen ($\varphi = 38\%$) brought about a 35% drop in ventilation and a 1°C increase in temperature. The screens also influence the vertical temperature distribution inside a greenhouse in that the lower the porosity the greater the vertical gradient, and the higher the temperature with height (Soni *et al*., 2005).

The negative effect of insect-proof screens on the natural ventilation and interior microclimate of greenhouses, which also has a negative effect on crop growth and development (Kittas *et al*., 2002; Teitel, 2010), can be exacerbated by the accumulation of dust on the mesh structure. This effect has received scant attention, and the only reference found to date is the study by Linker *et al*. (2002). These authors found that two months after the installation of a 50 mesh screen in a greenhouse of 50 $m^2$, the pressure drop coefficient of the mesh increased from 12 to 200. The term mesh refers to the number of threads per inch in the densest direction of the mesh. This term is not suitable for an insect-proof screen as it makes no mention of the other direction of the threads. Although it does not provide sufficient information on the geometric characteristics of the mesh, this term has been used in numerous scientific articles (*e.g.* Fatnassi *et al*., 2000; Linker *et al*., 2002; Dayan *et al*., 2004; Katsoulas *et al*., 2006).

Knowledge of the geometric characteristics of insect-proof screens is of the utmost importance,

especially in studies related to the screens' effects on microclimate and/or insect population inside the greenhouse. In most of the scientific studies concerning insect-proof screens consulted, scant information is provided; usually the thread density (in mesh or indicating the number of weft and warp threads per square centimeter) and the porosity. Very few works indicate other important parameters such as the thread diameter and the pore size. With a view to obtaining the geometric characteristics of the screens, the present study uses innovative software developed by the University of Almería. This software was used in a previous work to ascertain the geometric characteristics of 41 different types of insect-proof screens, and the results were highly satisfactory (Valera *et al*., 2003; Álvarez *et al*., 2006 and 2012; Álvarez, 2010).

A wide variety of insect-proof screens are available on the market. High density polyethylene is the most commonly used material in the manufacture of such screens (Fernández & Salgado, 2006), and additives are often used to protect the screen against ultraviolet radiation. The different types of screen that are currently commercially available differ from each other in characteristics such as porosity (the ratio between open area and total area), mesh size, thread dimension (diameter or thickness), texture (woven, knitted, woven/knitted), colour and light transmission (Teitel, 2007). The screens may be translucid (crystal), photoselective, or in different colours (black, green, etc.). Photoselective screens are used in order to make difficult for insects to identify their host plants (Antignus, 2000).

The present work has analysed the geometric characteristics of four insect-proof screens. They were analysed when new, prior to installation in two experimental greenhouses, and after several years of usage they were analysed once again. This study aims, therefore, to analyse the influence of the screens' deterioration due to the passage of time and the accumulation of dust and dirt on the geometric characteristics of insect-proof screens.

## Material and methods

### Experimental setup

The insect-proof screens analysed were installed in the side vents of two multi-span greenhouses located at the agricultural research farm belonging to the University of Almería (Fig. 1), in south-eastern Spain (36° 51' N, 02° 16' W and 87 masl). Both naturally-ventilated greenhouses, greenhouse 1 (24 × 45 m$^2$) and greenhouse 2 (18 × 45 m$^2$), were divided in half by a polyethylene sheet, which allowed us to study the inside microclimate of the two halves separately, and to install different insect-proof screens in each half.

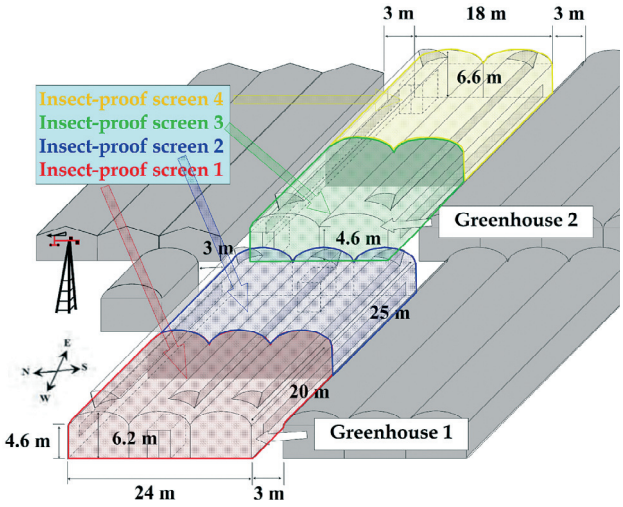


**Figure 1.** Distribution of the insect-proof screens in the two greenhouses.

Natural ventilation in greenhouse 1 consisted of two continuous side vents and three continuous roof vents, as opposed to two continuous side vents and two continuous roof vents in greenhouse 2 (Fig. 1). The dimensions of the vents of the two greenhouses and the values of the ventilation surface (when all vents are completely open) are specified in Table 1. For thorough information of the technology with which these greenhouses are equipped, see López *et al.* (2012).

Four different insect-proof screens were placed on the side vents of the sectors of the test greenhouses (Table 2). Screens 1 and 2 were installed in August 2007, and screens 3 and 4 in September 2008. All four were removed from the greenhouses in September 2011.

Mesh 1 is an experimental mesh with a thread density of 13 × 30 threads cm$^{-2}$ designed by the Engineering Department of the University of Almería and manufactured by a collaborating company. Meshes 2, 3 and 4 are commercial models distributed by a local firm, all with a thread density of 10 × 20 threads cm$^{-2}$ (Table 2). All meshes are made with HDPE threads;

**Table 1.** Dimensions of the vents and values of maximum ventilation surface $S_V/S_A$ (maximum vent surface / ground surface) for the two greenhouses

| | Section | Northern side vent (m²) | Southern side vent (m²) | Roof vent (m²) | Ground surface (m²) | $S_V/S_A$ (%) |
|---|---|---|---|---|---|---|
| Greenhouse 1 | Western | 1.05 × 17.5 | 1.05 × 17.5 | 0.97 × 17.5 (×3) | 24 × 20 | 18.3 |
| | Eastern | 1.05 × 22.5 | 1.05 × 22.5 | 0.97 × 22.5 (×3) | 24 × 25 | 18.8 |
| Greenhouse 2 | Western | 1.05 × 15.0[1] | 1.05 × 17.5 | 0.97 × 17.5 (×2) | 18 × 20 | 18.9 |
| | Eastern | 1.05 × 20.0[1] | 1.05 × 22.5 | 0.97 × 22.5 (×2) | 18 × 25 | 19.6 |

[1] The length of these vents is lower due to the presence of two antechambers in the northern side of the greenhouse (Fig. 1a).

**Table 2.** Original insect-proof screens placed in the greenhouse vents

| | Section | Number | $D_f$[1] | Type | Thread material | Installation date | Removal date |
|---|---|---|---|---|---|---|---|
| Greenhouse 1 | Western | Screen 1 | 13 × 30 | Crystal | HDPE [2] | Aug. 2007 | Sept. 2011 |
| | Eastern | Screen 2 | 10 × 20 | Crystal | HDPE | | |
| Greenhouse 2 | Western | Screen 3 | 10 × 20 | Photoselective | HDPE | Sept. 2008 | Sept. 2011 |
| | Eastern | Screen 4 | 10 × 20 | Crystal | HDPE | | |

[1] $D_f$: thread densities (threads cm$^{-2}$) according to the manufacturer Criado y López S.L. (El Ejido, Spain). [2] HDPE: high density polyethylene.

meshes 1, 2 and 4 are made with crystal threads and mesh 3 is made with photoselective threads.

The screens were installed on the side vents of two multi-tunnel Mediterranean greenhouses. The mechanisms used to hold the screens in place did not contribute to their deterioration. U-shaped (*omega*) metal frames were attached to the vent structure, and the mesh was then inserted and held in place by polyethylene stoppers (Figs. 2a and 2b). The mesh is not subjected to movement of any type that may affect its structure during usage. Indeed, the structure of the threads in the mesh is unaltered over time, unlike that of the mesh in Almería-type greenhouses, in which the roof and side walls are formed by two networks of manually interwoven galvanized wire. This wire structure is used to support the plastic covering, and the insect-proof screens are placed between the wire structures and held in place by means of wire ties (Fig. 2c).

In order to determine screen's geometric characteristics the following analyses were carried out: (a) before installation the new insect-proof screens were analysed by digital imagery to determine their two-dimensional characteristics; (b) after removal the dirty old insect-proof screens were analysed by digital imagery to determine the estimated imaging porosity ($\varphi^*$); (c) after removal the old screens were washed and then analysed by digital imagery to determine the $\varphi^*$ and the two-dimensional geometric characteristics.

## Bidimensional geometric characterisation

For geometric characterisation of the insect-proof screens a specific software tool was used (Valera *et al*., 2003; Álvarez *et al*., 2006 and 2012; Álvarez, 2010). This software allows the screens' geometric characteristics to be obtained from digital images. The images in question were taken with a Motic DMWB1-223 microscope (Motic Spain S.L., Barcelona, Spain) equipped with a digital camera using Motic Images Plus 2.0 software (Motic Spain S.L., Barcelona). The 4x microscope lens was calibrated, obtaining a resolution of 10.5 μm pixel$^{-1}$. Three random samples were taken from each screen and placed between two microscope slides. A surface of 2 cm$^2$ was drawn on one of the microscope slides, and this corresponded to the approximate area analysed. Using the 4x lens, each image taken corresponds to a surface of 0.34 × 0.25 cm$^2$. For each sample 24 images were taken, *i.e.* the total surface area analysed was 2.04 cm$^2$ for each sample. The procedure was as follows:

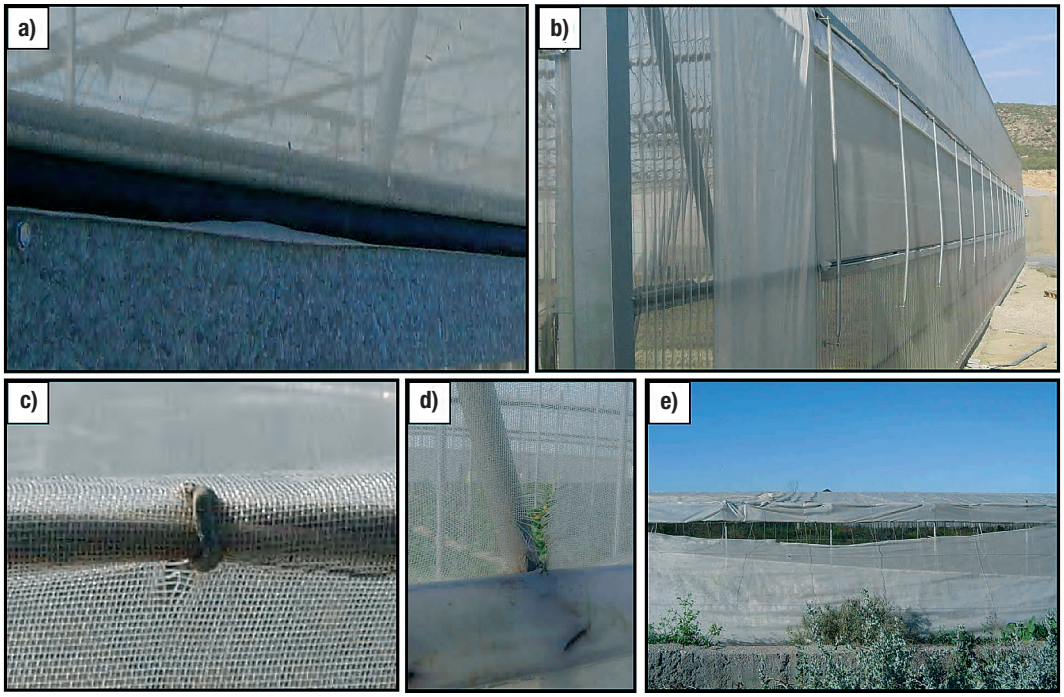


**Figure 2.** Mounting of the mesh on the *omega* frame in a multi-span Mediterranean greenhouse (a and b), tear in the mesh caused by the wire tie in an Almería-type greenhouse (c), rip in an insect-proof screen originated from a wire tie (d), and detachment of the insect-proof screen due to tears at several consecutive wire ties (e).

I. Take colour digital images of each sample (Fig. 3a). In order to process the digital images they must first be converted to black and white images.

II. Conversion from colour to black and white images. As the threads of the screen are opaque, the white area of the image, corresponding to the pore, must first be converted from white to grey (Fig. 3b). Based on this image, the software transforms the image to black and white, the threads appear black and the pores white (Fig. 3c).

III. Identification of the pore vertices (Fig. 3d). The software identifies the vertices of the pores (Valera *et al*., 2003; Álvarez, 2010; Álvarez *et al*., 2006 and 2012), occasionally requiring manual correction or identification of the vertex.

IV. Obtaining geometric data. Once the vertices of all the pores have been correctly identified, the software determines the density of the threads (number of weft and warp threads per $cm^2$), the porosity $\varphi$ ($m^2\ m^{-2}$), the average diameter of the threads $D_h$ (μm) and the parameters showed in Fig. 4.

This method of analysis based on digital images taken by a microscope was described by Álvarez *et al*. (2012). These authors analysed the reliability of this method comparing the geometric values measured using the software with those calculated from the manufacturer's data. The greatest differences for $L_{px}$ and $L_{py}$ were 0.7 and 3.8 μm, respectively; for the mean value of porosity the difference was 0.2% (Álvarez *et al*., 2012).

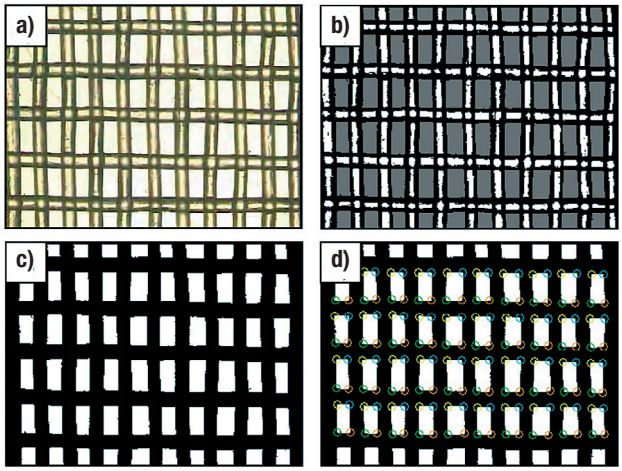


**Figure 3.** Images of a mesh sample: taken with the microscope (a), processed with grey pores (b), converted to black and white (c) and with the vertices identified (d).

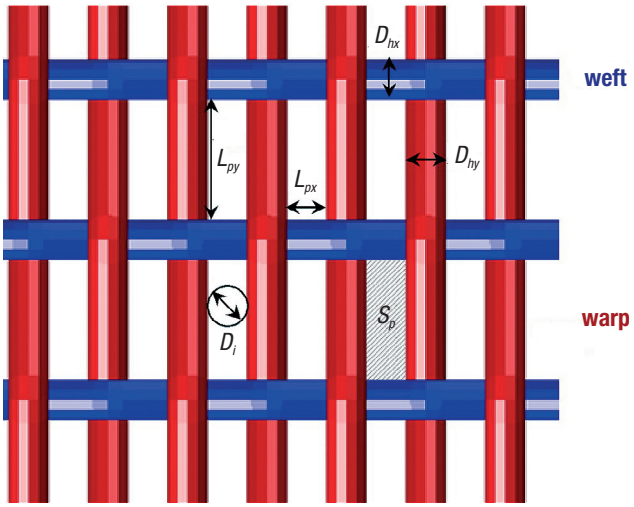


**Figure 4.** Geometric parameters determined using the software (Valera *et al*., 2003; Álvarez *et al*., 2006 and 2012; Álvarez, 2010). $L_{px}$ and $L_{py}$, the lengths of the pore (μm) in the direction of the weft and warp, respectively; $D_{hx}$ and $D_{hy}$, diameter (μm) of the weft and warp threads, respectively; $D_i$, diameter of the inside circumference of the pore (μm); $S_p$, area of the pore ($mm^2$).

The designation of weft and warp comes from the textile industry, and these screens are flat woven on looms. The weft refers to the threads that are fixed on the loom and determine, therefore, the width of the mesh. The weft threads are divided into two groups of threads that are separated alternately in order to permit the shuttle to pass between them carrying the warp threads and thus weaving the fabric.

### Estimated imaging porosity (white pixel vs black pixel)

The two-dimensional geometric characterization carried out by the software provides the porosity of the mesh φ ($m^2\ m^{-2}$), defined as the area of the pores $S_p$ compared to the total surface area $S_t$ as considered by Valera *et al*. (2003), Álvarez *et al*. (2006 and 2012) and Álvarez (2010):

$$\varphi = \frac{S_p}{S_t} = \frac{L_{px} L_{py}}{\left(L_{px} + D_{hy}\right)\left(L_{py} + D_{hx}\right)} \quad [1]$$

When the analysis procedure is applied to dirty screens (Fig. 5a), the vertices identified do not correspond to the real geometry of the pores (Fig. 5b), and consequently the two-dimensional characteristics cannot be obtained correctly. In such cases it was decided to determine the so-called *estimated imaging porosity* ($\varphi^*$), based on the black and white images of the screen samples (Fig. 5b), dividing the total number of white pixels in the image (corresponding to the pores) by the total of black ones (corresponding to the threads). The value of the parameter $\varphi^*$ differs from the correct value of porosity φ determined using the software.

In order to determine the statistical differences between geometric parameters, multiple range tests were carried out applying Fisher's least significant difference (LSD), establishing the confidence level at 99%, with Statgraphics Plus for Windows 4.1 (Manugistics Inc., Rockville, MD, USA).

## Results and discussion

The first results described are the differences in the two-dimensional geometric parameters obtained by the software between the new and old (washed) screens after 3-4 years of use. Then estimates of the loss of porosity due to the accumulation of dust are presented and the combination of both effects on screen porosity is quantified.

### Two-dimensional geometric characteristics (deterioration of the screens)

After washing the old screens and eliminating the accumulated dirt, it might be expected that the geometric characteristics would not vary from those obtained when the newly purchased screens were analysed. However, possibly due to deterioration of the threads over time, the thread diameter was found to have increased in all four screens analysed, and the differences were statistically significant. The mean diameter of the threads $D_h$ increased by 2.6% in mesh 1, 3.9% in meshes 2 and 3, and 2.1% in mesh 4. Insect-proof screens are exposed to ultraviolet radiation and adverse climatological conditions during use, and these may lead to deterioration of the thread molecular structure.

As the diameter of the threads increases, there is a slight increase in the density of threads in the mesh, and the dimensions of the pores is reduced in both directions ($L_{px}$ and $L_{py}$). Consequently the pore area ($S_p$) is smaller, and the final porosity of the screen (φ) is diminished (Table 3).

**Table 3.** Geometric characteristics of the new screens (New) and the old washed screens (Old). Average value and standard deviation of: φ, porosity ($m^2\ m^{-2}$); $L_{px}$ and $L_{py}$, the lengths of the pore (μm) in the direction of the weft and warp, respectively; $D_{hx}$ and $D_{hy}$, diameter (μm) of the weft and warp threads, respectively; $D_h$, diameter of the threads (μm); $D_i$, diameter of the inside circumference of the pore (μm); $S_p$, area of the pore ($mm^2$).

| *N* | | $D_r$ | φ | $L_{px}$ | $L_{py}$ | $D_{hx}$ | $D_{hy}$ | $D_h$ | $D_i$ | $S_p$ |
|---|---|---|---|---|---|---|---|---|---|---|
| 1 | New | 13.1 × 30.5 | 0.390 ± 0.006 | 164.6 ± 9.3 | 593.3 ± 19.0 | 168.6 ± 6.6 | 163.1 ± 6.3 | 165.5 ± 7.0 | 167.4 ± 9.6 | 0.098 ± 0.006 |
| | Old | 13.4 × 30.7 | 0.371 ± 0.006 | 156.5 ± 10.7 | 574.6 ± 19.3 | 170.5 ± 6.0 | 169.3 ± 6.0 | 169.8 ± 6.0 | 159.7 ± 10.8 | 0.090 ± 0.007 |
| 2 | New | 9.9 × 19.7 | 0.335 ± 0.011 | 233.7 ± 23.9 | 734.0 ± 29.2 | 276.4 ± 11.2 | 273.4 ± 10.7 | 274.5 ± 11.0 | 236.6 ± 24.0 | 0.171 ± 0.019 |
| | Old | 10.0 × 20.2 | 0.300 ± 0.011 | 208.3 ± 23.8 | 719.90 ± 41.2 | 283.0 ± 9.7 | 286.6 ± 10.4 | 285.3 ± 10.3 | 212.2 ± 23.9 | 0.150 ± 0.019 |
| 3 | New | 9.2 × 20.7 | 0.375 ± 0.007 | 234.9 ± 16.1 | 838.7 ± 27.0 | 245.8 ± 7.1 | 248.0 ± 8.3 | 247.2 ± 7.9 | 238.7 ± 16.4 | 0.197 ± 0.015 |
| | Old | 9.2 × 20.7 | 0.355 ± 0.004 | 225.8 ± 16.2 | 828.4 ± 22.5 | 257.0 ± 5.3 | 256.9 ± 8.7 | 256.9 ± 7.6 | 231.6 ± 16.5 | 0.187 ± 0.014 |
| 4 | New | 10.1 × 20.0 | 0.379 ± 0.007 | 256.6 ± 14.3 | 736.4 ± 17.1 | 256.8 ± 8.3* | 243.7 ± 8.2 | 248.6 ± 10.4 | 259.8 ± 14.4 | 0.189 ± 0.011 |
| | Old | 10.3 × 20.2 | 0.359 ± 0.011 | 244.1 ± 15.6 | 716.0 ± 23.0 | 256.7 ± 11.2* | 252.3 ± 9.4 | 253.9 ± 10.3 | 246.7 ± 15.8 | 0.174 ± 0.013 |

*N*: number of the screen; $D_r$: thread density (threads $cm^{-2}$). *No statistically significant differences at the 99.0% confidence level.

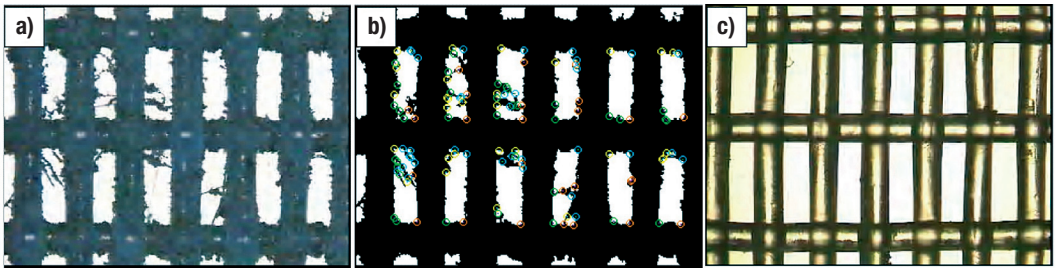


**Figure 5.** Images corresponding to mesh 2: microscope image of the old, dirty mesh (a), processed image with the vertices identified (b) and microscope image of the new sample (c).

**Table 4.** Average values (average value ± standard deviation) of the estimated imaging porosity, $\varphi^*$ ($m^2\ m^{-2}$), and the porosity, φ ($m^2\ m^{-2}$), determined by the software

| *N* | Estimated imaging porosity, $\varphi^*$ | | Software porosity, φ | |
|---|---|---|---|---|
| | Old and dirty | Old and washed | Old and washed | New |
| 1 | 0.299 ± 0.031 | 0.347 ± 0.008 | 0.371 ± 0.006 | 0.390 ± 0.006 |
| 2 | 0.214 ± 0.011 | 0.289 ± 0.012 | 0.300 ± 0.011 | 0.335 ± 0.011 |
| 3 | 0.288 ± 0.011 | 0.333 ± 0.006 | 0.355 ± 0.004 | 0.375 ± 0.007 |
| 4 | 0.253 ± 0.021 | 0.347 ± 0.016 | 0.359 ± 0.011 | 0.379 ± 0.007 |

*N*: screen number.

The length of the pore in the weft direction ($L_{px}$) drops by 4.9% in meshes 1 and 4, and by 10.9% and 3.9% in meshes 2 and 3, respectively. In the warp direction the length ($L_{py}$) decreases by 3.2%, 1.9%, 1.2% and 2.8% in meshes 1, 2, 3 and 4, respectively. The mean area of the pores ($S_p$) drops by 8.2%, 12.3%, 5.1% and 7.9% in meshes 1, 2, 3 and 4, respectively.

In short, the most important final effect to bear in mind is the reduction in porosity of the screen. The deterioration of the mesh structure over time results in losses of porosity φ of 4.9% (mesh 1), 10.4% (mesh 2) and 5.3% (meshes 3 and 4). Therefore, the pressure drop coefficient observed by Linker *et al*. (2002) due to the accumulation of dust is also affected by this deterioration of the mesh.

## Changes in screen porosity (deterioration + dirt)

In order to ascertain the reduction in porosity of the screens due to the accumulation of dust and dirt, the $\varphi^*$ was calculated (Table 4). This parameter is obtained

considering the reference surface area $S_t$ equal to the size of the digital images of the screens/meshes/samples. To obtain accurate values of porosity the reference surface area $S_t$ must be selected in such a way as to maintain the correct proportion between the surface corresponding to the threads and that of the pores (Álvarez *et al*., 2012). This was only possible by identifying the vertices of the pores using the software on clean meshes. Particles of dirt on the old meshes (Fig. 5a) prevent correct location of the pore vertices (Fig. 5b), thus making it impossible for the software to select the reference surface area $S_t$. Both values of porosity ($\varphi$ and $\varphi^*$) have been calculated for old, washed screens, and the value of $\varphi^*$ was found to be lower than the value of $\varphi$ in all cases; this difference is due to the incorrect selection of $S_t$ in the case of $\varphi^*$. Both parameters are related using the following expression $\varphi = 1.131\ \varphi^* - 0.026$ ($R^2 = 0.97$ and $p$-value = 0.016), statistically significant at the 95% confidence level.

Bearing in mind the error made when calculating the $\varphi^*$, this parameter has been determined for the old, dirty screens and for the same samples after washing with abundant water (Table 4).

The reduction in the $\varphi^*$ was determined as 13.8% for mesh 1, 26.0% for mesh 2, 13.5% for mesh 3 and 27.1% for mesh 4. These percentages include two effects: the accumulation of dust and dirt, and the deterioration of the threads. Previously, the reduction in porosity caused by the increase in diameter of the threads was calculated as 4.9% (mesh 1), 10.4% (mesh 2) and 5.3% (meshes 3 and 4). It can therefore be calculated that the reduction in the $\varphi^*$ caused solely by the accumulation of dirt is 8.9%, 15.6%, 8.2% and 21.8% for meshes 1, 2, 3 and 4, respectively.

Given the relationship between $\varphi$ obtained by the software and the $\varphi^*$ presented before, and knowing the values of $\varphi^*$ for the old, dirty screens, the correct values of porosity $\varphi$ can be calculated.

This methodology has allowed us to measure $\varphi$ for the old, dirty screens, obtaining values of 0.312, 0.216, 0.300 and 0.260 for meshes 1, 2, 3 and 4, respectively. Therefore the reduction in porosity $\varphi$ is estimated at 20.0%, 35.5%, 20.1% and 31.4% for meshes 1 to 4, respectively. Likewise, if we subtract from these values the effect of deterioration of the threads, we obtain the following values of reduction of porosity $\varphi$ due to the accumulation of dust and dirt: 15.1%, 25.1%, 14.8% and 26.1% for meshes 1 to 4, respectively.

The loss of porosity observed in these analyses is mainly due to the accumulation of dust and dirt (mean reduction in porosity for the four screens of 20.3%), and to a lesser extent to the deterioration of the threads (mean reduction in porosity for the four screens of 6.5%). The mechanism used to hold the screens in these experimental greenhouses (Figs. 2a-b) did not contribute to their deterioration (Fig. 5c), unlike that of the mesh in Almería-type greenhouses, in which the roof and side walls are formed by two networks of manually interwoven galvanized wire. As mentioned this wire structure is used to support the plastic covering, and the insect-proof screens are placed between the wire structures and held in place by means of wire ties (Fig. 2c). These ties require perforation of both the plastic covering and the insect-proof screen, and result in breakage and tearing of the mesh (Fig. 2d), mainly due to buffeting by the wind. These tears can even lead to the screens becoming completely unattached (Fig. 2e), leaving the greenhouse completely unprotected. This tearing has not been observed in the screens in our experimental greenhouses due to the better system used to hold them in place (Figs. 2a-b). It is extremely important that the system employed to hold the insect-proof screens in place should not contribute to their deterioration over time.

As remarked in the Introduction, many researchers have demonstrated the negative effect of insect-proof screens on greenhouse natural ventilation and microclimate. These negative effects are worsened considerably by the accumulation of dust and the deterioration of the mesh, as is confirmed by the major reduction in porosity that has been quantified in the present analysis. Given the increase in thread diameter and the consequent decrease in porosity of the mesh, further in-depth studies are required to determine the useful life of these agro-textiles.

Regarding the accumulation of dust and dirt in the pores of the insect-proof screens, we recommend that they should be washed with water at high pressure at least once a month. It is worth recalling that Linker *et al*. (2002) estimated that after two months the pressure drop coefficient of a 50-mesh screen had increased from 12 to 200. The frequency of washing will depend on the meteorological and geographical conditions of each region. The characteristic strong winds in the semi-arid province of Almería carry large quantities of dust, and so the insect-proof screens require frequent washing.

The results obtained in the present work are conditioned by the warm, semi-arid Mediterranean climate. The area where the greenhouses are located

has a maximum 24-hour precipitation of under 100 mm (data from 1950-1985), 2800-3000 hours of sunlight per year (Capel, 1990) and a maximum absolute monthly temperature of 37.5 ± 2.9 in the month of July (De Leon *et al.,* 1989). The results of the present study should be considered bearing in mind the specific climatic conditions prevalent in south-eastern Spain. The quantitative results obtained cannot be directly extrapolated to zones with different climatic conditions.

As final conclusions, analysis of the geometric characteristics of insect-proof screens before installation and after several years of use has revealed two negative effects. The first is that with time the structure of the mesh deteriorates, the thread diameter ($D_h$) increases by an average of 3.1%. This implies a mean reduction in the pore dimensions of 6.2% and 2.3% in the weft ($L_{px}$) and warp ($L_{py}$) directions respectively, and consequently the mean area of the pores ($S_p$) is reduced by 8.4%. In short, the porosity of the screen (φ) suffers a mean reduction of 6.5%, and the maximum reduction value was 10.4% for screen 2. The second negative effect is the accumulation of dust and dirt in the insect-proof screens gives rise to a mean reduction in porosity (φ) of the insect-proof screens of 20.3%, the lowest reduction was 14.8% (screen 3) and the maximum was 26.1% (screen 4). The combined total of these two negative effects amounted to a 26.8% mean reduction in porosity (φ). The lowest value observed was 20.0% (screen 1), corresponding to a porosity of 0.390 for the new mesh as opposed to 0.312 for the dirty, used mesh. The highest reduction in porosity recorded was 35.5% (screen 2), corresponding to porosity values of 0.335 for the new screen and 0.216 for the used one. It is recommended that insect-proof screens installed on greenhouse vents should be washed at least once a month with high pressure water.

## Acknowledgements

This work has been financed by the *Junta de Andalucía* and the *Ministerio de Ciencia e Innovación* by means of research grants P09-AGR-4593 and AGL2010-22284-C03-01, respectively.

## References

Álvarez AJ, 2010. Estudio de las características geométricas y del comportamiento aerodinámico de las mallas antiinsectos utilizadas en los invernaderos como medida de protección vegetal. Doctoral thesis. Universidad de Almería, Almería, Spain [In Spanish].

Álvarez AJ, Valera DL, Molina FD, 2006. A method for the analysis of the geometric characteristics of protection screens. Acta Hort 719: 557-564.

Álvarez AJ, Oliva RM, Valera DL, 2012. Software for the geometric characterisation of insect-proof screens. Comput Electron Agric 82: 134-144.

Antignus Y, 2000. Manupulation of wavelength-dependent behaviour of insects: an IPM tool to impede insects and restrict epidemics of insect-borne viruses. Virus Res 71: 213-220.

Baeza EJ, Pérez-Parra JJ, Montero JI, Bailey BJ, López JC, Gázquez JC, 2009. Analysis of the role of sidewall vents on buoyancy-driven natural ventilation in parral-type greenhouses with and without insect screens using computational fluid dynamics. Biosyst Eng 104: 86-96.

Baker JR, Jones RK, 1989. Screening as part of insect and disease management in the greenhouse. N.C. Flower Growers' Bulletin 34: 1-9.

Bartzanas T, Boulard T, Kittas C, 2002. Numerical simulation of the airflow and temperature distribution in a tunnel greenhouse equipped with insect-proof screen in the openings. Comput Electron Agric 34: 207-221.

Berlinger MJ, Mordechl S, Leeper A, 1991. Application of screens to prevent whitefly penetration into greenhouses in the Mediterranean Basin. Proc of the Working Group Integrated Control in Protecting Crops under Mediterranean Climate, Alassio (Italy), Sept 29-Oct 2, pp: 105-110.

Berlinger MJ, Leblush-Mordechl S, Fridja D, Mor N, 1992. The effect of types of greenhouse screens on the presence of western flower thrips: a preliminary study. OILB-SROP Bulletin 16(2): 13-19.

BOJA, 2007. Reglamento Específico de Producción Integrada de Cultivos Hortícolas Protegidos. Boletín Oficial de la Junta de Andalucía 211 [In Spanish].

Capel JJ, 1990. Climatología de Almería. Cuadernos monográficos 7. Diputación Provincial de Almería, Instituto de Estudios Almerienses, Almería, Spain [In Spanish].

Dayan J, Dayan E, Strassberg Y, Presnov E, 2004. Simulation and control of ventilation rates in greenhouses. Math Comput Simulat 65: 3-17.

De Leon A, Arriba A, De la Plaza MC, 1989. Caracterización agroclimática de la provincia de Almería. Ministerio de Agricultura, Pesca y Alimentación, Madrid, Spain [In Spanish].

Dierickx IE, 1998. Flow reduction of synthetic screens obtained with both a water and airflow apparatus. J Agr Eng Res 71: 67-73.

Fatnassi H, Boulard T, Demrati H, Bouirden L, Sappe G, 2002. Ventilation performance of a large Canarian-type greenhouse equipped with insect-proof nets. Biosyst Eng 82(1): 97-105.

Fatnassi H, Boulard T, Bouirden L, 2003. Simulation of climatic conditions in full-scale greenhouse fitted with insect-proof screens. Agric Forest Meteorol 118: 97-111.

Fatnassi H, Boulard T, Poncet C, Chave M, 2006. Optimisation of greenhouse insect screening with computational fluid dynamics. Biosyst Eng 93(3): 301-312.

Harmanto, Tantau H, Salokhe VM, 2006. Microclimate and air exchange rates in greenhouses covered with different nets in the humid tropics. Biosyst Eng 94(2): 239-253.

Katsoulas N, Bartzanas T, Boulard T, Mermier M, Kittas C, 2006. Effect of vent openings and insect screens on greenhouse ventilation. Biosyst Eng 93(4): 427-436.

Kittas C, Boulard T, Bartzanas T, Katsoulas N, Mermier M, 2002. Influence of an insect screen on greenhouse ventilation. T ASAE 45(4): 1083-1090.

Kittas C, Katsoulas N, Bartzanas T, Mermier M, Boulard T, 2008. The impact of insect screens and ventilation openings on the greenhouse microclimate. T ASABE 51(6): 2151-2165.

Linker R, Tarnopolsky M, Seginer I, 2002. Increased resistance to flow and temperature-rise resulting from dust accumulation on greenhouse insect-proof screens. ASAE Annual International Meeting, Chicago (USA), Jun 28-31, 9 pp.

López A, Valera DL, Molina-Aiz FD, Peña A, 2012. Sonic anemometry to evaluate airflow characteristics and temperature distribution in empty Mediterranean greenhouses equipped with pad-fan and fog systems. Biosyst Eng 113: 334-350.

Miguel AF, Silva AM, 2000. Porous materials to control climate behaviour of enclosures: an application to the study of screened greenhouses. Energ Buildings 31: 195-209.

Miguel AF, Van de Braak NJ, Bot GPA, 1997. Analysis of the airflow characteristics of greenhouse screening materials. J Agr Eng Res 67: 105-112.

Muñoz P, Montero JI, Antón A, Giuffrida F, 1999. Effect of insect-proof screens and roof openings on greenhouse ventilation. J Agr Eng Res 73: 171-178.

Smith KM, 1972. Plant virus diseases. Academic Press, NY, USA. 684 pp.

Soni P, Salokhe VM, Tantau HJ, 2005. Effect of screen mesh size on vertical temperature distribution in naturally ventilated tropical greenhouses. Biosyst Eng 92(4): 469-482.

Taylor RAJ, Shalhevet S, Spharim I, Berlinger MJ, Lebiush-Mordechi S, 2001. Economic evaluation of insect-proof screens for preventing tomato yellow leaf curl virus of tomatoes in Israel. Crop Prot 20: 561-569.

Teitel M, 2007. The effect of screened openings on greenhouse microclimate. Agric Forest Meteorol 143(3-4): 159-175.

Teitel M, 2010. Using computational fluid dynamics simulations to determine pressure drops on woven screens. Biosyst Eng 105: 172-179.

Valera DL, Álvarez AJ, Molina FD, Peña A, López JA, Madueño A, 2003. Caracterización geométrica de diferentes tipos de agrotextiles utilizados en invernaderos. II Congreso Nacional de Agroingeniería, AG03-0722: 670-675, Córdoba (Spain) [In Spanish].

Valera DL, Molina FD, Álvarez AJ, López JA, Terrés-Nicoli JM, Madueño A, 2005. Contribution to characterization of insect-proof screens: experimental measurements in wind tunnel and CFD simulation. Acta Hort 691: 441-448.

Valera DL, Álvarez AJ, Molina FD, 2006. Aerodynamic analysis of several insect-proof screens used in greenhouses. Span J Agric Res 4(4): 273-279.